

Underdetermined DOA Estimation Under the Compressive Sensing Framework: A Review

Qing Shen, Wei Liu*, Wei Cui*, and Siliang Wu

Abstract—Direction of arrival (DOA) estimation from the perspective of sparse signal representation has attracted tremendous attention in past years, where the underlying spatial sparsity reconstruction problem is linked to the compressive sensing (CS) framework. Although this is an area with ongoing intensive research and new methods and results are reported regularly, it is time to have a review about the basic approaches and methods for CS-based DOA estimation, in particular for the underdetermined case. We start from the basic time-domain CS-based formulation for narrowband arrays and then move to the case for recently developed methods for sparse arrays based on the co-array concept. After introducing two specifically designed structures (the two-level nested array and the co-prime array) for optimizing the virtual sensors corresponding to the difference co-array, this CS-based DOA estimation approach is extended to the wideband case by employing the group sparsity concept, where a much larger physical aperture can be achieved by allowing a larger unit inter-element spacing and therefore leading to further improved performance. Finally, a specifically designed ULA structure with associated CS-based underdetermined DOA estimation is presented to exploit the difference co-array concept in the spatio-spectral domain, leading to a significant increase in DOFs. Representative simulation results for typical narrowband and wideband scenarios are provided to demonstrate their performance.

Index Terms—Compressive sensing, direction of arrival estimation, underdetermined, difference co-array, sparse array structures.

I. INTRODUCTION

Direction of arrival (DOA) estimation, as a fundamental problem in array signal processing [1]–[4], has been studied extensively over the past decades, playing a very important role in various applications including radar, sonar, speech enhancement and wireless communications, etc. Many high-resolution methods such as MUSIC [5], ESPRIT [6], and their extensions including Tensor-MUSIC [7], Tensor-ESPRIT [8], and Tensor-MODE [9] have been proposed for narrowband DOA estimation. Very recently, DOA estimation in the presence of nonuniform noise was studied in [10]. For the wideband case, some representative methods include the incoherent signal subspace method (ISSM) [11], the coherent signal

subspace method (CSSM) [12], and the test of orthogonality of projected subspaces (TOPS) method [13].

In the past few years, DOA estimation has attracted further attention due to its connection with the theory of sparse signal representation, where the underlying spatial sparsity reconstruction problem is linked to the compressive sensing (CS) framework [14], [15]. Compared with those aforementioned traditional estimation methods, performing DOA estimation from the perspective of sparse signal reconstruction bring benefits such as smaller number of data samples required, lower sensitivity to SNR, and ability to deal with highly correlated and coherent sources. In [16], a CS-based scheme is applied to DOA estimation with a single snapshot and a reduced dimension method called ℓ_1 -SVD is proposed for multiple snapshots. A lot of applications related to the direction finding problem under the CS framework has been investigated [16]–[22], and the performance analysis with both lower bounds and upper bounds on the probability of incorrect sparse support recovery is studied in [23]. DOA estimation based on a sparse representation of array covariance vectors with a presented explicit error-suppression criterion is proposed in [24], but the computational complexity is extremely high by jointly recovering the sparsest coefficients corresponding to the DOAs. In [25], DOA estimation through Bayesian compressive sensing strategies is proposed, and a novel compressive MUSIC algorithm is presented in [26]. In [27], sparse spectrum fitting (SpSF) for DOA estimation is proposed, which is proved to be asymptotically consistent for infinite number of snapshots.

Among the studied DOA estimation problems, the case for which the number of sources is larger than the number of physical sensors has proved to be much more difficult [28]–[30]. For such an underdetermined DOA estimation task, various sparse array structures have been proposed as possible solutions [31]–[35]. Recently, two classes of sparse arrays, namely nested arrays and co-prime arrays, have been proposed [36]–[38]. A virtual array structure with increased number of virtual uniform linear array (ULA) sensors is generated based on the difference co-array concept, leading to an increased number of degrees of freedom (DOFs) which can be exploited for DOA estimation. Apart from the spatial smoothing based subspace approaches [36]–[40], signal reconstruction methods under the CS framework based on the difference co-array concept are employed for narrowband DOA estimation [41]–

* Corresponding authors.

Q. Shen, W. Cui and S. Wu are with the School of Information and Electronics, Beijing Institute of Technology, Beijing, 100081, China (e-mail: qing-shen@outlook.com; cuiwei@bit.edu.cn; siliangw@bit.edu.cn).

W. Liu is with the Department of Electronic and Electrical Engineering, University of Sheffield, Sheffield, S1 3JD, UK (e-mail: w.liu@sheffield.ac.uk).

[45], and the performance of sparse support recovery using correlation information is analyzed in [46]. A novel sparse reconstruction method is proposed for DOA estimation of a mixture of coherent and uncorrelated targets using active nonuniform arrays [47], where a virtual array with sensors distributed at the difference co-array of the sum co-array is generated, offering significant enhancement in DOFs based on the co-array equivalence. Furthermore, super nested arrays are proposed in [48], [49] to reduce mutual coupling, and high-order difference co-arrays are employed in [50]–[52] to further increase the DOFs with limited physical sensors. Then in [53], group sparsity based DOA estimation methods for wideband co-prime arrays with reduced computational complexity is proposed, allowing a much larger unit inter-element spacing than the standard co-prime array and therefore leading to further improved performance. In fact, these CS-based underdetermined DOA estimation methods employing the co-array equivalence principle can be applied to arbitrary linear arrays.

For both aforementioned classes of sparse arrays, at least two uniform linear sub-arrays are needed in their configurations to optimize the virtual sensor positions corresponding to the difference co-array. In [42], [54], a single ULA is used with two continuous-wave signals of co-prime frequencies. Instead of employing two uniform linear sub-arrays, the single ULA acts as two equivalent sub-arrays in a co-prime array structure at the two co-prime frequencies and CS-based DOA estimation method is employed to handle the underdetermined DOA estimation problem. The idea with multiple frequencies is further considered in [55]–[57], and the same philosophy applies for the detection of multiple-frequency sources, assuming that the signal DOAs remain unchanged across all the frequency band. Then in [58], it is extended to the wideband case and a novel design for wideband ULAs with associated group sparsity based sparse signal reconstruction method exploiting the difference co-array concept in the spatio-spectral domain is proposed. The linear frequency modulated continuous wave (LFMCW) signal is chosen as the transmitted waveform to ensure the correlation characteristic among different frequencies of the received signals, which is required for difference co-array generation in the spatio-spectral domain. With a specifically designed ULA structure according to the frequency band of interest, a significantly increased number of detectable targets is achieved by employing the group sparsity based wideband DOA estimation method across multiple frequency pairs.

One common issue with CS-based DOA estimation is the dictionary mismatch problem, i.e. DOAs of the source signals may not exactly fall onto the values of the finite search grid [59]–[62]. One straightforward solution to this problem is to use a denser search grid with a smaller step size. However, this increases the computational complexity of the optimisation

process significantly. One solution is to adaptively refine the search grid only around the region where the sources are located [16], [62], while a joint sparse recovery method is developed for underdetermined off-grid DOA estimation of narrowband signals in [63], [64], with a two-step off-grid approach proposed in [65] for the wideband case.

Motivated by these rich research results under the CS framework for DOA estimation, especially for underdetermined DOA estimation, in this paper, we first review DOA estimation with sensor arrays from the perspective of sparse signal reconstruction in the time domain [16]. Due to the high complexity introduced by the estimation approach for multiple snapshots, the difference co-array based DOA estimation method is then extended to arbitrary linear arrays, where the CS-based sparse signal reconstruction method is applied to exploit the increased DOFs only available in the signal and noise power domain. Then two specifically designed classes of sparse arrays (nested arrays [36] and co-prime arrays [37], [38]) are presented, optimizing the virtual sensor positions corresponding to the difference co-array. Secondly, the CS-based DOA estimation method is extended to the wideband case based on the group sparsity concept, and except for all the advantages shared by DOA estimation under the CS framework, this group sparsity based wideband method is capable of allowing a much larger unit inter-element spacing, translated to a further improved performance. Finally, with a specifically designed ULA structure where LFMCW signal is chosen as the transmitted waveform, an associated underdetermined DOA estimation method under the CS framework is presented to exploit the difference co-array concept in the spatio-spectral domain, leading to a significant increase in DOFs.

This review paper is organized as follows. The review on the time domain DOA estimation and the difference co-array based DOA estimation under the CS framework with specifically designed sparse array structures are presented in Section II. The group sparsity based sparse signal reconstruction method for the wideband case is introduced in Section III, where further performance improvement with large unit spacing is also presented. The method for wideband ULAs employing the difference co-array concept in the spatio-spectral domain is studied in Section IV. Representative simulation results demonstrating the performance of the reviewed DOA estimation methods are provided in Section V, and conclusions are drawn in Section VI.

II. NARROWBAND DOA ESTIMATION UNDER THE CS FRAMEWORK

A. Narrowband signal model

Consider an N -sensor arbitrary linear array with its sensor positions distributed in the set S , expressed as

$$S = \{\alpha_0 \cdot d, \alpha_1 \cdot d, \dots, \alpha_{N-1} \cdot d\}, \quad (1)$$

where d is the unit spacing, $\alpha_n \cdot d$ is the position of the n -th sensor, $0 \leq n \leq N - 1 \cap n \in \mathbf{Z}$, and \mathbf{Z} is the set of all integers.

Assume that there are K mutually uncorrelated far-field narrowband signals $s_k(t)$ impinging from incident angles $\theta_k, k = 1, 2, \dots, K$, respectively. After sampling with a frequency f_s , we use $\mathbf{x}[i]$ to represent the observed discrete signal vector, and the narrowband array output model in discrete form is given by

$$\mathbf{x}[i] = \mathbf{A}(\boldsymbol{\theta})\mathbf{s}[i] + \bar{\mathbf{n}}[i], \quad (2)$$

where the source signal vector $\mathbf{s}[i] = [s_1[i], \dots, s_K[i]]$, and $\bar{\mathbf{n}}[i]$ is the vector for spatially white noise. The steering matrix $\mathbf{A}(\boldsymbol{\theta}) = [\mathbf{a}(\theta_1), \dots, \mathbf{a}(\theta_K)]$, with each column vector $\mathbf{a}(\theta_k)$ as the steering vector corresponding to the k -th source signal, expressed as

$$\mathbf{a}(\theta_k) = \left[e^{-j\frac{2\pi\alpha_0 d}{\lambda} \sin(\theta_k)}, \dots, e^{-j\frac{2\pi\alpha_{N-1} d}{\lambda} \sin(\theta_k)} \right]^T, \quad (3)$$

where λ is the signal wavelength and $\{\cdot\}^T$ represents the transpose operation.

B. CS-based DOA estimation for a single snapshot

For the i -th snapshot, the CS based signal reconstruction approach is employed to explore the advantages of the sparse distribution of the spatial source signals [16]. A search grid of K_g ($K_g \gg K$) potential incident angles $\theta_{g,0}, \dots, \theta_{g,K_g-1}$ is first generated, and an overcomplete representation of $\mathbf{A}(\boldsymbol{\theta})$ is then constructed, given by

$$\mathbf{A}(\boldsymbol{\theta}_g) = [\mathbf{a}(\theta_{g,0}), \dots, \mathbf{a}(\theta_{g,K_g-1})]. \quad (4)$$

It is noted that in $\mathbf{A}(\boldsymbol{\theta}_g)$, the steering vector at each column corresponds to one potential incident angle. In this framework, the constructed steering matrix $\mathbf{A}(\boldsymbol{\theta}_g)$ is independent of the actual source directions $\boldsymbol{\theta}$.

We also construct a $K_g \times 1$ column vector $\mathbf{s}_g[i]$, with each entry representing a potential source signal at the corresponding incident angle. Then, the signal model from the perspective of sparse signal reconstruction can be updated to

$$\mathbf{x}[i] = \mathbf{A}(\boldsymbol{\theta}_g)\mathbf{s}_g[i] + \bar{\mathbf{n}}[i]. \quad (5)$$

The estimation problem can be solved by the following constrained optimisation:

$$\begin{aligned} \min \quad & \|\mathbf{s}_g[i]\|_0 \\ \text{subject to} \quad & \|\mathbf{x}[i] - \mathbf{A}(\boldsymbol{\theta}_g)\mathbf{s}_g[i]\|_2 \leq \varepsilon \end{aligned} \quad (6)$$

where $\|\cdot\|_0$ is the ℓ_0 norm, $\|\cdot\|_2$ represents the ℓ_2 norm, and ε is the allowable error bound.

Due to difficulty in solving the ℓ_0 norm based problem in (6), an ℓ_1 norm is employed instead as an approximation [16],

[66], and the CS-based DOA estimation for a single snapshot can be finally formulated as [16]

$$\begin{aligned} \min \quad & \|\mathbf{s}_g[i]\|_1 \\ \text{subject to} \quad & \|\mathbf{x}[i] - \mathbf{A}(\boldsymbol{\theta}_g)\mathbf{s}_g[i]\|_2 \leq \varepsilon \end{aligned} \quad (7)$$

where $\|\cdot\|_1$ is the ℓ_1 norm. The entries in $\mathbf{s}_g[i]$ represent the DOA results over K_g search grids.

Different from ℓ_0 norm which uniformly penalises all non-zero valued coefficients, the ℓ_1 norm penalises larger weight coefficients more heavily than smaller ones. To make the ℓ_1 norm a closer approximation to the ℓ_0 norm, a reweighted ℓ_1 norm minimisation method can be adopted here [67]–[70], where a larger weighting term is introduced to those coefficients with smaller non-zero values and a smaller weighting term to those coefficients with larger non-zero values. This weighting term will change according to the resultant coefficients at each iteration. This iterative reweighted ℓ_1 minimization approach can be applied to all ℓ_1 norm based formulation in this review paper.

C. CS-based DOA estimation for multiple snapshots

When multiple data snapshots are available, we could perform DOA estimation by (7) for each snapshot i and then combine these independent estimates by some kind of averaging/fusion to obtain a more accurate result. However, a more effective approach to achieve higher accuracy and robustness to noise is to jointly estimate the DOA of the impinging signals across multiple snapshots employing the group sparsity concept, since they all have the same spatial support.

Denote $\mathbf{X} = [\mathbf{x}[0], \dots, \mathbf{x}[P-1]]$, where P is the number of snapshots. Similarly, we can define $\mathbf{S} = [\mathbf{s}[0], \dots, \mathbf{s}[P-1]]$ and $\bar{\mathbf{N}} = [\bar{\mathbf{n}}[0], \dots, \bar{\mathbf{n}}[P-1]]$. Then the signal model for multiple snapshots can be obtained by

$$\mathbf{X} = \mathbf{A}(\boldsymbol{\theta})\mathbf{S} + \bar{\mathbf{N}}, \quad (8)$$

Note that the matrix \mathbf{S} is not generally sparse in time domain. To introduce spatial sparsity in the formulation, similar to the single-snapshot case, we construct $\mathbf{S}_g = [\mathbf{s}_g[0], \dots, \mathbf{s}_g[P-1]]$, and use the row vector $\mathbf{s}_{g,k_g}, 0 \leq k_g \leq K_g - 1$ to represent the k_g -th row of the matrix \mathbf{S}_g . Then a new $K_g \times 1$ column vector is generated by performing ℓ_2 norm to each row in \mathbf{S}_g , expressed as

$$\hat{\mathbf{s}}_g = [\|\mathbf{s}_{g,0}\|_2, \|\mathbf{s}_{g,1}\|_2, \dots, \|\mathbf{s}_{g,K_g-1}\|_2]^T. \quad (9)$$

Finally the CS-based optimization problem for multiple snapshots can be formulated as [16]

$$\begin{aligned} \min \quad & \|\hat{\mathbf{s}}_g\|_1 \\ \text{subject to} \quad & \|\tilde{\mathbf{x}} - \mathbf{A}(\boldsymbol{\theta})\bar{\mathbf{s}}_g\|_2 \leq \varepsilon, \end{aligned} \quad (10)$$

where $\tilde{\mathbf{x}} = \text{vec}\{\mathbf{X}\}$ and $\bar{\mathbf{s}}_g = \text{vec}\{\mathbf{S}_g\}$ with $\text{vec}\{\cdot\}$ representing the vectorizing operation. The column vector $\hat{\mathbf{s}}_g$ are

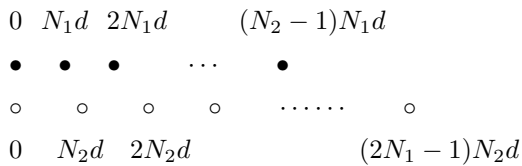


Fig. 2. Structure of a general co-prime array, consisting of two sub-arrays with the shared 0-th sensor.

spacing between adjacent physical sensors, while there are N_2 sensors in the second sub-array starting from the position $(N_1 + 1)d$ with the inter-element spacing $(N_1 + 1)d$. The number of physical sensors in a two-level nested array is $N_1 + N_2$, and the achieved difference co-array lags in the set Φ_S is expressed as

$$\Phi_S = \{\mu, -N_2(N_1 + 1) + 1 \leq \mu \leq N_2(N_1 + 1) - 1\}. \quad (17)$$

From the virtual array perspective based on the difference co-array concept, a ULA with $2N_2(N_1 + 1) - 1$ virtual sensors can be generated corresponding to the consecutive integers from $-N_2(N_1 + 1) + 1$ to $N_2(N_1 + 1) - 1$ in Φ_S , leading to a significant increase in DOFs by employing the DOA estimation method introduced in (16).

Co-prime arrays are another class of sparse arrays designed for DOFs improvement based on the difference co-array concept. There are also two uniform linear sub-arrays in a standard co-prime array. For a given unit spacing d , the first sub-array has N_2 sensors with an inter-element spacing of N_1d , while the second sub-array has $2N_1$ sensors with N_2d as its spacing between adjacent sensors. As shown Fig. 2, the sensor at the zeroth position is shared by the two sub-arrays. Therefore, there are $2N_1 + N_2 - 1$ sensors in total.

According to [37], [53], the difference co-array lags in Φ_S of a standard co-prime array can reach every integer from $-N_1N_2$ to N_1N_2 , corresponding to a virtual ULA of $2N_1N_2 + 1$ sensors with an increased number of DOFs. Furthermore, there are several non-consecutive lags in the set Φ_S , and it has been verified in [45] that the CS-based DOA estimation method can achieve a better performance compared with the spatial smoothing based subspace method due to the exploration of all the unique lags.

There are several structure extensions based on the standard co-prime arrays, such as two generalized extensions based on the standard co-prime arrays introduced in [45], namely co-prime arrays with compressed inter-element spacing (CACIS) and co-prime arrays with displaced sub-array (CADiS). However, for all array structures designed for optimising the difference co-array lags, the CS-based DOA estimation method employing the difference co-array concept (16) can be applied with good performance achieved.

Remarks on the Cramér-Rao Bounds (CRB) for sparse arrays: It is noted that for the overdetermined case (less sources

than physical sensors), the root mean square error (RMSE) of MUSIC will converge to zero as input SNR tends to infinity. However, for the underdetermined case, according to **Theorem 4** in [71], the CRB has an asymptotic expression which does not decay to zero for sufficiently large SNR as SNR tends to infinity. This Theorem is also verified by the numerical results provided in [71], [72], and the performance result of our discussed underdetermined DOA estimation method provided in Section V is consistent with the analysis in [71], [72].

III. WIDEBAND DOA ESTIMATION UNDER THE CS FRAMEWORK

A. Wideband signal model

Consider the same N -sensor arbitrary linear array with its sensor positions distributed in the set S as given in (1). Assume that there are K mutually uncorrelated far-field wideband signals $s_k(t)$ impinging from incident angles $\theta_k, k = 1, 2, \dots, K$, respectively. Then, the signals observed from the n -th sensor of the given array structure can be expressed as

$$x_n(t) = \sum_{k=1}^K s_k [t - \tau_n(\theta_k)] + \bar{n}_n(t), \quad (18)$$

where $0 \leq n \leq N - 1$. Take the zeroth position of the given array as the reference. Then we have $\tau_0(\theta_k) = 0$. $\tau_n(\theta_k)$ represents the time delay of the k -th impinging signal from incident angle θ_k arriving at the n -th sensor, and $\bar{n}_n(t)$ is the white Gaussian noise at the corresponding sensor.

After sampling with a frequency f_s , an L -point discrete Fourier transform (DFT) is applied. The array output model in the DFT domain can be expressed as

$$\mathbf{X}[l, p] = \mathbf{A}(l, \boldsymbol{\theta})\mathbf{S}[l, p] + \bar{\mathbf{N}}[l, p], \quad (19)$$

where $\mathbf{X}[l, p]$ is the observed signal vector at the l -th frequency bin, $\mathbf{S}[l, p]$ is a column vector holding all signals at the l -th frequency bin, and $\bar{\mathbf{N}}[l, p]$ is the noise vector. $\mathbf{A}(l, \boldsymbol{\theta}) = [\mathbf{a}(l, \theta_1), \dots, \mathbf{a}(l, \theta_K)]$ represent the steering matrix at frequency f_l corresponding to the l -th frequency bin, with each column vector $\mathbf{a}(l, \theta_k)$ representing the steering vector corresponding to the k -th source signal at frequency f_l , expressed as

$$\mathbf{a}(l, \theta_k) = \left[e^{-j\frac{2\pi\alpha_0 d}{\lambda_l} \sin(\theta_k)}, \dots, e^{-j\frac{2\pi\alpha_{N-1} d}{\lambda_l} \sin(\theta_k)} \right]^T, \quad (20)$$

where $\lambda_l = c/f_l$ and c is the wave propagation speed.

B. Group sparsity based wideband DOA estimation

To exploit the increased DOFs introduced by the difference co-array, we first generate a virtual array corresponding to the

difference co-array. For the l -th frequency bin, the correlation matrix is calculated by

$$\begin{aligned} \mathbf{R}_{\text{xx}}[l] &= \text{E} \{ \mathbf{X}[l, p] \cdot \mathbf{X}^H[l, p] \} \\ &= \sum_{k=1}^K \sigma_k^2[l] \mathbf{a}(l, \theta_k) \mathbf{a}^H(l, \theta_k) + \sigma_n^2[l] \mathbf{I}_N, \end{aligned} \quad (21)$$

where $\sigma_k^2[l]$ is the power of the k -th impinging signal at the l -th frequency bin, and $\sigma_n^2[l]$ represents the corresponding noise power. In practice, the correlation matrix $\mathbf{R}_{\text{xx}}[l]$ can be estimated within P samples in each frequency bin.

Then the virtual array with sensors corresponding to the difference co-array is obtained by vectorizing $\mathbf{R}_{\text{xx}}[l]$, given as

$$\begin{aligned} \mathbf{z}[l] &= \text{vec} \{ \mathbf{R}_{\text{xx}}[l] \} = \tilde{\mathbf{A}}[l] \tilde{\mathbf{s}}[l] + \sigma_n^2[l] \tilde{\mathbf{I}}_{N^2} \\ &= \tilde{\mathbf{A}}^\circ[l] \tilde{\mathbf{s}}^\circ[l], \end{aligned} \quad (22)$$

with

$$\begin{aligned} \tilde{\mathbf{A}}^\circ[l] &= [\tilde{\mathbf{A}}[l], \tilde{\mathbf{I}}_{N^2}], \\ \tilde{\mathbf{s}}^\circ[l] &= [\tilde{\mathbf{s}}^T[l], \sigma_n^2[l]]^T, \end{aligned}$$

where the equivalent steering matrix of the generated virtual array $\tilde{\mathbf{A}}[l] = [\tilde{\mathbf{a}}(l, \theta_1), \dots, \tilde{\mathbf{a}}(l, \theta_K)]$ with each column vector $\tilde{\mathbf{a}}(l, \theta_k) = \mathbf{a}^*(l, \theta_k) \otimes \mathbf{a}(l, \theta_k)$ representing the corresponding steering vector, and the equivalent source signals $\tilde{\mathbf{s}}[l] = [\sigma_1^2[l], \dots, \sigma_K^2[l]]^T$.

With a generated search grid of K_g potential incident angles $\theta_{g,0}, \dots, \theta_{g,K_g-1}$, an overcomplete representation of the equivalent steering matrix is constructed by $\tilde{\mathbf{A}}_g[l] = [\tilde{\mathbf{a}}(l, \theta_{g,0}), \dots, \tilde{\mathbf{a}}(l, \theta_{g,K_g-1})]$. Denote $\tilde{\mathbf{A}}_g^\circ[l] = [\tilde{\mathbf{A}}_g[l], \tilde{\mathbf{I}}_{N^2}^2]$ and $\tilde{\mathbf{s}}_g^\circ[l] = [\tilde{\mathbf{s}}_g^T[l], \sigma_n^2[l]]^T$, where the column vector $\tilde{\mathbf{s}}_g[l]$ has K_g elements with each being a potential source signal at the corresponding incident angle.

Then the CS-based narrowband DOA estimation method in (16) can be applied to the l -th frequency bin, given by [43], [53]

$$\begin{aligned} \min \quad & \|\tilde{\mathbf{s}}_g^\circ[l]\|_1 \\ \text{subject to} \quad & \|\mathbf{z}[l] - \tilde{\mathbf{A}}_g^\circ[l] \tilde{\mathbf{s}}_g^\circ[l]\|_2 \leq \varepsilon. \end{aligned} \quad (23)$$

Instead of combining the DOA estimation results across the entire frequency range of interest to obtain the final DOA, a more effective approach is to estimate the wideband DOA across all frequency bins of interest simultaneously based on the group sparsity concept, in the same way as in the narrowband case with multiple snapshots. Due to the same spatial support, a better performance and higher accuracy can be achieved.

Assume that the bandwidth of the impinging source signals covers Q frequency bins in the DFT domain, where $Q \leq L$. We use l_q , $0 \leq q \leq Q-1$, to represent the index of these interested frequency bins, and l_q may or may not be adjacent to each other. With the same search grid of K_g potential incident

angles for different frequency bins, a block diagonal matrix $\tilde{\mathbf{B}}_g^\circ$ is generated using $\tilde{\mathbf{A}}_g^\circ[l_q]$, expressed as

$$\tilde{\mathbf{B}}_g^\circ = \text{blkdiag} \left\{ \tilde{\mathbf{A}}_g^\circ[l_0], \tilde{\mathbf{A}}_g^\circ[l_1], \dots, \tilde{\mathbf{A}}_g^\circ[l_{Q-1}] \right\}. \quad (24)$$

Another matrix \mathbf{U}_g° with size of $(K_g + 1) \times Q$ is then constructed, given as

$$\mathbf{U}_g^\circ = [\tilde{\mathbf{s}}_g^\circ[l_0], \tilde{\mathbf{s}}_g^\circ[l_1], \dots, \tilde{\mathbf{s}}_g^\circ[l_{Q-1}]]. \quad (25)$$

Denote row vector \mathbf{u}_{g,k_g}° , $0 \leq k_g \leq K_g$, as the k_g -th row of the matrix \mathbf{U}_g° . By performing ℓ_2 norm to each row vector \mathbf{u}_{g,k_g}° , a new column vector is formed as

$$\hat{\mathbf{u}}_g^\circ = [\|\mathbf{u}_{g,0}^\circ\|_2, \dots, \|\mathbf{u}_{g,K_g}^\circ\|_2]^T. \quad (26)$$

Finally, the wideband DOA estimation method employing the group sparsity concept is formulated as follows

$$\begin{aligned} \min_{\hat{\mathbf{u}}_g^\circ} \quad & \|\hat{\mathbf{u}}_g^\circ\|_1 \\ \text{subject to} \quad & \|\tilde{\mathbf{z}} - \tilde{\mathbf{B}}_g^\circ \hat{\mathbf{u}}_g^\circ\|_2 \leq \varepsilon, \end{aligned} \quad (27)$$

where $\tilde{\mathbf{z}} = [\mathbf{z}^T[l_0], \dots, \mathbf{z}^T[l_{Q-1}]]^T$, and $\hat{\mathbf{u}}_g^\circ$ is obtained by vectorizing \mathbf{U}_g° , expressed as $\hat{\mathbf{u}}_g^\circ = \text{vec}(\mathbf{U}_g^\circ)$. The first K_g elements of the column vector $\hat{\mathbf{u}}_g^\circ$ are the corresponding wideband DOA estimation results over the K_g search grids.

The main drawback of the group sparsity based method is its high computational complexity. In [53], the redundant entries are combined together to form a formulation with significantly reduced dimension for low-complexity wideband DOA estimation.

C. Performance improvement with large unit spacing employing the group sparsity based wideband DOA estimation method

Normally, the unit spacing should satisfy the relationship of $d \leq \lambda_{\min}/2$ to avoid spatial aliasing, where λ_{\min} is the minimum wavelength within the frequency range of interest. However, the unit spacing d is able to be larger than $\lambda_{\min}/2$, while accurate DOA results without spatial aliasing could still be obtained by applying the group sparsity based wideband DOA estimation method in (27).

For the wideband case, the aliasing locations are different at different frequency bins. The group sparsity based wideband method is capable of forcing a common sparsity location across the entire frequency band simultaneously, corresponding to the true incident angles of the impinging source signals under the same spatial sparsity. Therefore, a larger unit spacing can be achieved compared with the standard array structure when performing the group sparsity based method, leading to a larger physical array aperture as well as a larger virtual array aperture, and finally translated to better performance with more accurate estimation results.

However, we expect that there is a threshold value, and the estimation performance will degrade when the unit spacing

is larger than the threshold. We can still perform the group sparsity based DOA estimation effectively at $d = \lambda_{\max}/2$ with λ_{\max} as the maximum wavelength within the frequency range, where the largest array aperture (both physical array aperture and the virtual array aperture) is achieved under the condition of no spatial aliasing only for the minimum frequency of interest.

IV. WIDEBAND DOA ESTIMATION FOR ULAS BASED ON THE DIFFERENCE CO-ARRAY CONCEPT

A. Signal model

For further increase in DOFs, a novel design for wideband ULAs with associated DOA estimation method under the CS framework based on the difference co-array concept in the spatio-spectral domain is proposed in [58], where only a single ULA structure is designed to achieve a larger number of detectable targets.

We consider applications such as radar, and the linear frequency modulated continuous wave (LFMCW) signal is chosen as the transmitted waveform to ensure the correlation characteristic among different frequencies of the received signals, and this characteristic is required for difference co-array generation in the spatio-spectral domain. The transmitted LFMCW signal is given as

$$s(t) = Ae^{j(2\pi f_c t + \pi \alpha \cdot \text{mod}(t+\tau, T)^2 + \varphi)}, \quad (28)$$

where A is the signal amplitude, f_c is an initial frequency, τ is an initial time-offset, and φ represents the initial phase. $\alpha = B/T$ is the chirp rate with B as the signal bandwidth and T as the modulation period. $\text{mod}(\cdot)$ is the modulo operator.

Consider an N -sensor ULA with the set of sensor positions S given by

$$S = \{n\tilde{d}, 0 \leq n \leq N-1, n \in \mathbf{Z}\}, \quad (29)$$

where \tilde{d} is the adjacent sensor spacing, and the design of \tilde{d} will be shown later.

Assume that there are K far-field targets distributed at incident angles θ_k , $k = 1, 2, \dots, K$, respectively. Then, the echo signals observed at the n -th sensor can be expressed as

$$x_n(t) = \sum_{k=1}^K \gamma_k(t) \cdot s[t - \tau_n(\theta_k)] + \bar{n}_n(t), \quad (30)$$

where the reflection coefficient $\gamma_k(t)$ is time-varying due to target motion or radar cross section (RCS) fluctuations, and it is in general frequency-dependent since the phase delay varies with frequency and the target reflectivity at different frequencies may be different.

After sampling with a frequency f_s and applying an L -point DFT, the array output model in the DFT domain is obtained, given as

$$\mathbf{X}[l, p] = \mathbf{A}(l, \boldsymbol{\theta})\mathbf{S}[l, p] + \bar{\mathbf{N}}[l, p], \quad (31)$$

where the model is similar to the one in (19), the only difference is that $\mathbf{S}[l, p] = [S_1[l, p], \dots, S_K[l, p]]^T$ is the column signal vector at the l -th frequency bin, with each entry $S_k[l, p]$ being the DFT of the p -th group discrete-time echo signals $\gamma_k[i]s[i]$.

Define $f_\Delta = f_s/L$ as the frequency interval between adjacent frequency bins. The spacing \tilde{d} between adjacent physical sensors is designed as

$$\tilde{d} = \frac{c}{2f_\Delta} \cdot \delta, \quad (32)$$

where δ is a variable used to adjust the spacing of the array. To avoid spatial aliasing, δ should be less than 1 according to the difference co-array concept in the spatio-spectral domain, and the best estimation performance is achieved at $\delta = 1$. Then, the steering vector $\mathbf{a}(l, \theta_k)$ corresponding to the l -th column vector in $\mathbf{A}(l, \boldsymbol{\theta})$ is expressed as

$$\mathbf{a}(l, \theta_k) = [1, e^{-j\pi l \delta \sin(\theta_k)}, \dots, e^{-j\pi(N-1)\delta \sin(\theta_k)}]^T. \quad (33)$$

B. Virtual array generation in the spatio-spectral domain

We also assume that the echo signal bandwidth covers Q frequency bins with the index of frequency bins $l_q \in \Phi_L$, $0 \leq q \leq Q-1$, where Φ_L is the set including Q frequency bin indexes. Then we select M frequency pairs, where the m -th, $0 \leq m \leq M-1$, pair consists of the frequency bins l_{m_1} and l_{m_2} with $l_{m_1}, l_{m_2} \in \Phi_L$. Then the auto-correlation matrices are calculated by

$$\begin{aligned} \mathbf{R}_{\mathbf{x}}[l_{m_1}, l_{m_1}] &= \mathbb{E} \{ \mathbf{X}[l_{m_1}, p] \cdot \mathbf{X}^H[l_{m_1}, p] \} \\ &= \sum_{k=1}^K \sigma_k^2[l_{m_1}, l_{m_1}] \mathbf{a}(l_{m_1}, \theta_k) \mathbf{a}^H(l_{m_1}, \theta_k) + \sigma_n^2[l_{m_1}, l_{m_1}] \mathbf{I}_N, \\ \mathbf{R}_{\mathbf{x}}[l_{m_2}, l_{m_2}] &= \mathbb{E} \{ \mathbf{X}[l_{m_2}, p] \cdot \mathbf{X}^H[l_{m_2}, p] \} \\ &= \sum_{k=1}^K \sigma_k^2[l_{m_2}, l_{m_2}] \mathbf{a}(l_{m_2}, \theta_k) \mathbf{a}^H(l_{m_2}, \theta_k) + \sigma_n^2[l_{m_2}, l_{m_2}] \mathbf{I}_N, \end{aligned}$$

where $\sigma_k^2[l_{m_1}, l_{m_1}]$ and $\sigma_k^2[l_{m_2}, l_{m_2}]$ represent the powers of the echo signal from the k -th target at the corresponding frequency bins, respectively, whereas $\sigma_n^2[l_{m_1}, l_{m_1}]$ and $\sigma_n^2[l_{m_2}, l_{m_2}]$ are the corresponding noise powers. These powers are all real and positive.

The cross-correlation matrices across the two frequency bins are shown as

$$\begin{aligned} \mathbf{R}_{\mathbf{x}}[l_{m_1}, l_{m_2}] &= \mathbb{E} \{ \mathbf{X}[l_{m_1}, p] \cdot \mathbf{X}^H[l_{m_2}, p] \} \\ &= \sum_{k=1}^K \sigma_k^2[l_{m_1}, l_{m_2}] \mathbf{a}(l_{m_1}, \theta_k) \mathbf{a}^H(l_{m_2}, \theta_k), \\ \mathbf{R}_{\mathbf{x}}[l_{m_2}, l_{m_1}] &= \mathbb{E} \{ \mathbf{X}[l_{m_2}, p] \cdot \mathbf{X}^H[l_{m_1}, p] \} \\ &= \sum_{k=1}^K \sigma_k^2[l_{m_2}, l_{m_1}] \mathbf{a}(l_{m_2}, \theta_k) \mathbf{a}^H(l_{m_1}, \theta_k). \end{aligned}$$

where owing to the phase shift between different frequencies caused by the LFMCW echo signal and the reflection component at different frequency, $\sigma_k^2[l_{m_1}, l_{m_2}]$ and $\sigma_k^2[l_{m_2}, l_{m_1}]$ are in general complex values. Note that $\mathbf{R}_x[l_{m_1}, l_{m_2}] = \mathbf{R}_x^H[l_{m_2}, l_{m_1}]$. Therefore, only the former one is used for DOA estimation.

Vectorizing these correlation matrices yields several virtual arrays, expressed as

$$\begin{aligned} \mathbf{z}[l_{m_1}, l_{m_1}] &= \text{vec} \{ \mathbf{R}_x[l_{m_1}, l_{m_1}] \} \\ &= \tilde{\mathbf{A}}[l_{m_1}, l_{m_1}] \tilde{\mathbf{s}}[l_{m_1}, l_{m_1}] + \sigma_n^2[l_{m_1}, l_{m_1}] \tilde{\mathbf{I}}_{N^2}, \\ \mathbf{z}[l_{m_2}, l_{m_2}] &= \text{vec} \{ \mathbf{R}_x[l_{m_2}, l_{m_2}] \} \\ &= \tilde{\mathbf{A}}[l_{m_2}, l_{m_2}] \tilde{\mathbf{s}}[l_{m_2}, l_{m_2}] + \sigma_n^2[l_{m_2}, l_{m_2}] \tilde{\mathbf{I}}_{N^2}, \\ \mathbf{z}[l_{m_1}, l_{m_2}] &= \text{vec} \{ \mathbf{R}_x[l_{m_1}, l_{m_2}] \} \\ &= \tilde{\mathbf{A}}[l_{m_1}, l_{m_2}] \tilde{\mathbf{s}}[l_{m_1}, l_{m_2}], \end{aligned}$$

with equivalent steering matrices

$$\begin{aligned} \tilde{\mathbf{A}}[l_{m_1}, l_{m_1}] &= [\tilde{\mathbf{a}}(l_{m_1}, l_{m_1}, \theta_1), \dots, \tilde{\mathbf{a}}(l_{m_1}, l_{m_1}, \theta_K)], \\ \tilde{\mathbf{A}}[l_{m_2}, l_{m_2}] &= [\tilde{\mathbf{a}}(l_{m_2}, l_{m_2}, \theta_1), \dots, \tilde{\mathbf{a}}(l_{m_2}, l_{m_2}, \theta_K)], \\ \tilde{\mathbf{A}}[l_{m_1}, l_{m_2}] &= [\tilde{\mathbf{a}}(l_{m_1}, l_{m_2}, \theta_1), \dots, \tilde{\mathbf{a}}(l_{m_1}, l_{m_2}, \theta_K)], \end{aligned}$$

where each column vector $\tilde{\mathbf{a}}(l_{m_1}, l_{m_1}, \theta_k) = \mathbf{a}^*(l_{m_1}, \theta_k) \otimes \mathbf{a}(l_{m_1}, \theta_k)$, $\tilde{\mathbf{a}}(l_{m_2}, l_{m_2}, \theta_k) = \mathbf{a}^*(l_{m_2}, \theta_k) \otimes \mathbf{a}(l_{m_2}, \theta_k)$, and $\tilde{\mathbf{a}}(l_{m_1}, l_{m_2}, \theta_k) = \mathbf{a}^*(l_{m_2}, \theta_k) \otimes \mathbf{a}(l_{m_1}, \theta_k)$. The equivalent signal vectors $\tilde{\mathbf{s}}[l_{m_1}, l_{m_1}] = [\sigma_1^2[l_{m_1}, l_{m_1}], \dots, \sigma_K^2[l_{m_1}, l_{m_1}]]^T$, $\tilde{\mathbf{s}}[l_{m_2}, l_{m_2}] = [\sigma_1^2[l_{m_2}, l_{m_2}], \dots, \sigma_K^2[l_{m_2}, l_{m_2}]]^T$, and $\tilde{\mathbf{s}}[l_{m_1}, l_{m_2}] = [\sigma_1^2[l_{m_1}, l_{m_2}], \dots, \sigma_K^2[l_{m_1}, l_{m_2}]]^T$.

Different difference co-array in the spatio-spectral domain can be obtained under different combinations of l_{m_1} and l_{m_2} , with the set of difference co-array lags achieving $\{\pm(l_{m_1}n_1 - l_{m_2}n_2), 0 \leq n_1, n_2 \leq N-1\}$. For special cases that l_{m_1} and l_{m_2} are chosen to be co-prime or nested, the received signals at the two frequency bins can be considered as signals received by a co-prime array or a nested array, and the increased DOFs can be exploited for DOA estimation.

C. Group sparsity based DOA estimation for a single frequency pair

For the m -th frequency pair with the same search grid of K_g potential incident angles, we generate the following matrices

$$\begin{aligned} \tilde{\mathbf{A}}_g[l_{m_1}, l_{m_1}] &= [\tilde{\mathbf{a}}(l_{m_1}, l_{m_1}, \theta_{g,0}), \dots, \tilde{\mathbf{a}}(l_{m_1}, l_{m_1}, \theta_{g,K_g-1})], \\ \tilde{\mathbf{A}}_g[l_{m_2}, l_{m_2}] &= [\tilde{\mathbf{a}}(l_{m_2}, l_{m_2}, \theta_{g,0}), \dots, \tilde{\mathbf{a}}(l_{m_2}, l_{m_2}, \theta_{g,K_g-1})], \\ \tilde{\mathbf{A}}_g[l_{m_1}, l_{m_2}] &= [\tilde{\mathbf{a}}(l_{m_1}, l_{m_2}, \theta_{g,0}), \dots, \tilde{\mathbf{a}}(l_{m_1}, l_{m_2}, \theta_{g,K_g-1})], \end{aligned}$$

and then a block diagonal matrix is constructed by $\tilde{\mathbf{A}}_g[m] = \text{blkdiag} \{ \tilde{\mathbf{A}}_g[l_{m_1}, l_{m_1}], \tilde{\mathbf{A}}_g[l_{m_2}, l_{m_2}], \tilde{\mathbf{A}}_g[l_{m_1}, l_{m_2}] \}$.

Denote $\mathbf{z}[m] = [\mathbf{z}^T[l_{m_1}, l_{m_1}], \mathbf{z}^T[l_{m_2}, l_{m_2}], \mathbf{z}^T[l_{m_1}, l_{m_2}]]^T$, and we construct a $K_g \times 3$ matrix $\tilde{\mathbf{S}}_g[m]$ with each column vector representing the potential source signals over the K_g

search grids. Then, according to the same spatial support, the following formulation can be obtained

$$\begin{aligned} \mathbf{z}[m] &= \tilde{\mathbf{A}}_g[m] \tilde{\mathbf{s}}_g[m] + \tilde{\mathbf{I}} \mathbf{w}[m] \\ &= \tilde{\mathbf{A}}_g^\circ[m] \tilde{\mathbf{s}}_g^\circ[m] \end{aligned} \quad (34)$$

where $\tilde{\mathbf{I}} = [\tilde{\mathbf{I}}_1, \tilde{\mathbf{I}}_2]$ is a $3N^2 \times 2$ matrix with $\tilde{\mathbf{I}}_1 = [\tilde{\mathbf{I}}_{N^2}^T, \mathbf{0}_{N^2}^T, \mathbf{0}_{N^2}^T]^T$ and $\tilde{\mathbf{I}}_2 = [\mathbf{0}_{N^2}^T, \tilde{\mathbf{I}}_{N^2}^T, \mathbf{0}_{N^2}^T]^T$ ($\mathbf{0}_{N^2}$ is a $N^2 \times 1$ column vector consisting of all zeros). $\tilde{\mathbf{s}}_g[m]$ is a $3K_g \times 1$ column vector obtained by vectorizing $\tilde{\mathbf{S}}_g[m]$, and $\mathbf{w}[m] = [\sigma_n^2[l_{m_1}, l_{m_1}], \sigma_n^2[l_{m_2}, l_{m_2}]]^T$. In addition, $\tilde{\mathbf{A}}_g^\circ[m] = [\tilde{\mathbf{A}}_g[m], \tilde{\mathbf{I}}]$ and $\tilde{\mathbf{s}}_g^\circ[m] = [\tilde{\mathbf{s}}_g[m], \mathbf{w}^T[m]]^T$.

Row vector $\mathbf{s}_{g,k_g}[m]$ is used to represent the k_g -th row of the matrix $\tilde{\mathbf{S}}_g[m]$. By performing ℓ_2 norm to each row, a new column vector is formed as given below

$$\hat{\mathbf{s}}_g[m] = [\|\mathbf{s}_{g,0}[m]\|_2, \|\mathbf{s}_{g,1}[m]\|_2, \dots, \|\mathbf{s}_{g,K_g-1}[m]\|_2]^T. \quad (35)$$

Then, the group sparsity based DOA estimation for a single frequency pair is formulated as [58]

$$\begin{aligned} \min_{\tilde{\mathbf{s}}_g^\circ[m]} \quad & \|\hat{\mathbf{s}}_g[m]\|_1 \\ \text{subject to} \quad & \|\mathbf{z}[m] - \tilde{\mathbf{A}}_g^\circ[m] \tilde{\mathbf{s}}_g^\circ[m]\|_2 \leq \varepsilon. \end{aligned} \quad (36)$$

D. Group sparsity based DOA estimation employing multiple frequency pairs

The group sparsity concept is expanded to jointly exploit multiple frequency pairs for wideband DOA estimation across the frequency band of interest.

For the selected M frequency pairs, a block diagonal matrix is generated by $\tilde{\mathbf{B}}_g^\circ = \text{blkdiag} \{ \tilde{\mathbf{A}}_g^\circ[0], \tilde{\mathbf{A}}_g^\circ[1], \dots, \tilde{\mathbf{A}}_g^\circ[M-1] \}$. Construct a $K_g \times 3M$ matrix \mathbf{U}_g and a $(3K_g + 2)M \times 1$ column vector \mathbf{u}_g° , given by

$$\begin{aligned} \mathbf{U}_g &= [\tilde{\mathbf{S}}_g[0], \tilde{\mathbf{S}}_g[1], \dots, \tilde{\mathbf{S}}_g[M-1]], \\ \mathbf{u}_g^\circ &= [\tilde{\mathbf{s}}_g^\circ[0], \tilde{\mathbf{s}}_g^\circ[1], \dots, \tilde{\mathbf{s}}_g^\circ[M-1]]^T. \end{aligned} \quad (37)$$

Based on the group sparsity concept, we define

$$\hat{\mathbf{u}}_g = [\|\mathbf{u}_{g,1}\|_2, \|\mathbf{u}_{g,2}\|_2, \dots, \|\mathbf{u}_{g,K_g}\|_2]^T, \quad (38)$$

with the row vector \mathbf{u}_{g,k_g} , $1 \leq k_g \leq K_g$ representing the k_g -th row of the matrix \mathbf{U}_g .

Finally, the wideband DOA estimation employing M frequency pairs is formulated as [58]

$$\begin{aligned} \min_{\mathbf{u}_g^\circ} \quad & \|\hat{\mathbf{u}}_g\|_1 \\ \text{subject to} \quad & \|\mathbf{z}_g - \tilde{\mathbf{B}}_g^\circ \mathbf{u}_g^\circ\|_2 \leq \varepsilon, \end{aligned} \quad (39)$$

where $\mathbf{z}_g = [\mathbf{z}^T[0], \mathbf{z}^T[1], \dots, \mathbf{z}^T[M-1]]^T$.

V. SIMULATION RESULTS

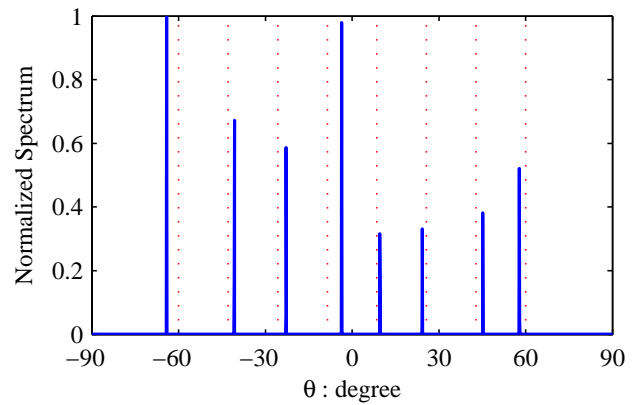
In this part, we provide some representative simulation results to show the performance of the discussed CS-based DOA estimation methods. There are K mutually uncorrelated far-field sources/targets with incident angles uniformly distributed from -60° to 60° , where different K is chosen for different examples. A search grid of $K_g = 3601$ potential incident angles is generated within the full range from -90° to 90° with a step size of 0.05° . The allowable error bound ε is chosen to give the best DOA estimation results through trial-and-error in every experiment. CVX, a software package for specifying and solving convex programs [73], [74], is used to solve all these optimisation problems in this section.

A. Narrowband DOA estimation results

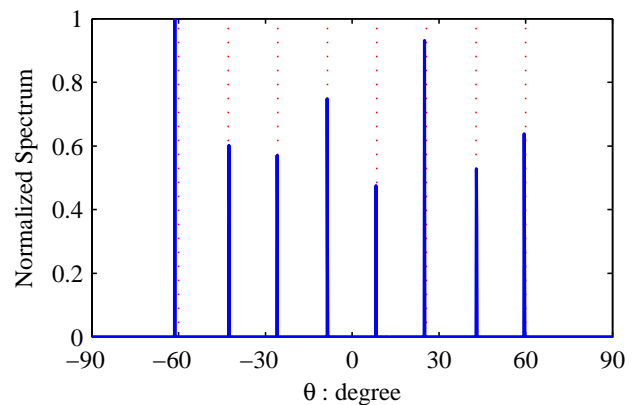
For the first set of simulations in this part, we consider a ULA with 9 sensors, and the unit spacing d is set to be $\lambda/2$. The input signal-to-noise ratio (SNR) is fixed at 0dB, and the number of sources $K = 8$. The DOA results obtained by the CS-based narrowband estimation method for a single snapshot (7) and the method exploiting multiple snapshots (10) is shown in Fig. 3, where the dotted lines represent the actual incident angles of the impinging source signals, while the solid lines represent the estimation results, and the number of snapshots P is set to be 100 for (10). Clearly, all the 8 sources have been distinguished successfully by the two methods.

In our second set of simulations in this part, we consider examples of two recently proposed classes of sparse arrays with $(N_1, N_2) = (4, 5)$ chosen for the two-level nested array and $(N_1, N_2) = (3, 4)$ chosen for the co-prime array. Then there are 9 physical sensors for both array structures. The DOA estimation method based on the difference co-array concept (16) is employed to find the DOAs, and the number of snapshots for estimating the correlation matrix $P = 1000$. With $K = 12$ sources, the DOA results are shown in Fig. 4. It is clear that for the underdetermined case, the difference co-array based DOA estimation method is capable of resolving all the 12 sources for both the two array structures with 9 sensors.

For the third set of simulations, we compare the estimation accuracy with respect to a varied input SNR through Monte Carlo simulations of 500 trials. We set the number of sources $K = 12$, and the number of snapshots $P = 1000$. The root mean square error (RMSE) results obtained by the CS-based method (16) and the spatial smoothing based MUSIC (SS-MUSIC) method [36]–[38], [50] with different array structures are shown in Fig. 5. Obviously, a higher estimation accuracy is achieved with a higher input SNR. The RMSEs with the two-level nested array consistently outperform the one with the co-prime array, since the physical array aperture of the nested array is $24d$, which is larger than the aperture of $20d$ for the co-prime array. Furthermore, it is clear that for the same array



(a) DOA estimation results of CS-based narrowband estimation method for a single snapshot.

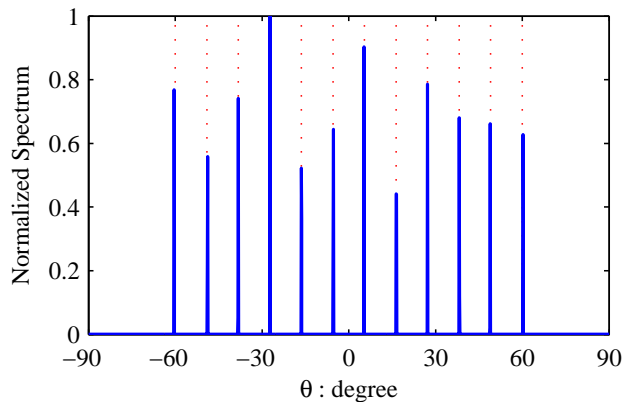


(b) DOA estimation results of CS-based narrowband estimation method for multiple snapshots.

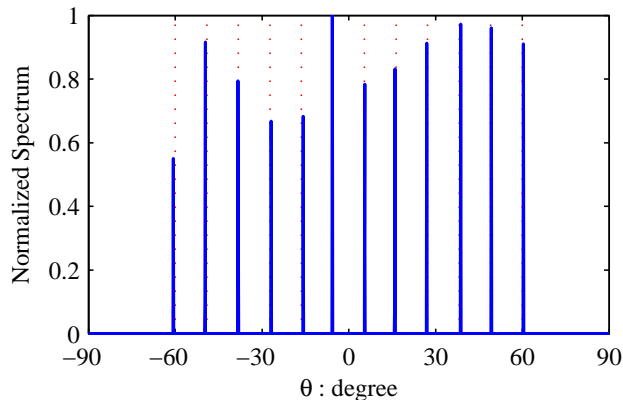
Fig. 3. Narrowband DOA estimation results obtained by the CS-based methods for a single snapshot and for multiple snapshots.

structure, the CS-based method outperforms the SS-MUSIC method for low input SNRs. For high input SNRs, the CS-based method and the SS-MUSIC share a similar performance for the nested array with the CS-based method being slightly more accurate, while much better performance can be achieved by the CS-based method for the co-prime array. It is noted that for the co-prime array there are non-consecutive integers in its set of difference co-array lags [45], [52], and the better performance of the CS-based method is due to exploration of all unique difference co-array lags including non-consecutive part, while the SS-MUSIC method only exploits the virtual ULA part.

For the fourth set of simulations, we fix the SNR to 0 dB, the number of sources is set to be $K = 12$, and the number of snapshots $P = 1000$. The sensitivity of the CS-based method (16) to the allowable error bound ε is explored based on the 9-sensor co-prime array with $(N_1, N_2) = (3, 4)$, as shown in Fig. 6. It is clear that the most accurate result can be obtained only around an appropriate value of ε . Roughly speaking, this appropriate value is related to the noise level of the system and also various array and data model errors in the convex



(a) DOA estimation results for a nested array.



(b) DOA estimation results for a co-prime array.

Fig. 4. Narrowband DOA estimation results obtained by the difference co-array based method for different structures.

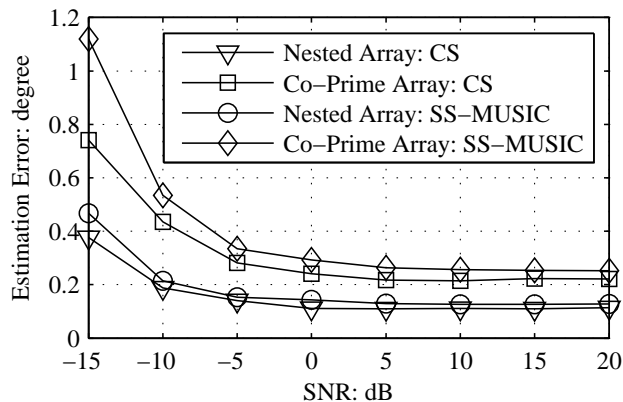


Fig. 5. RMSEs with different narrowband array structures versus input SNR.

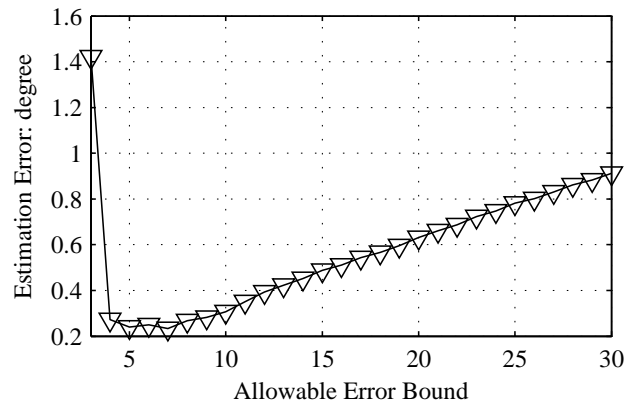


Fig. 6. RMSEs with respect to the allowable error bound.

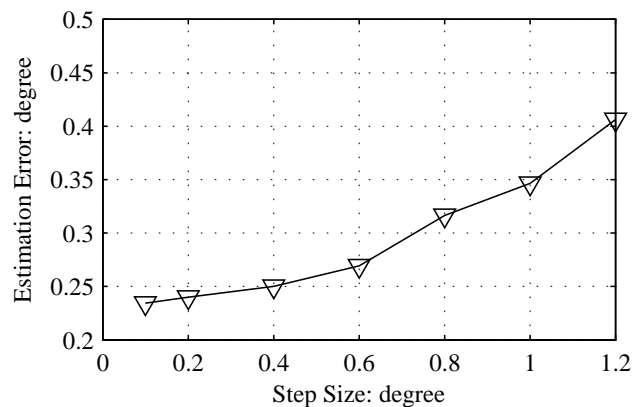


Fig. 7. RMSEs with respect to the step size.

optimization problem.

For the fifth set of simulations, we study the sensitivity of the CS-based method (16) to the step size r of the search grid. For different r , a search grid of $K_g = \frac{180}{r} + 1$ potential incident angles is generated within the full range from -90° to 90° . The input SNR is set to be 0 dB, while $K = 12$ and $P = 1000$. With the same co-prime array, the RMSE results versus step size r is shown in Fig. 7. Evidently, the performance becomes worse with the increase of the step size due to the dictionary mismatch problem caused by the off-grid sources whose true DOAs may not necessarily fall on the exact discrete finite grids.

Finally, with SNR fixed at 0 dB, $P = 1000$, and step size $r = 0.05$, the RMSE results with respect to the DOA separation \bar{h} between adjacent sources are shown in Fig. 8, where $K = 2$ uncorrelated far-field sources arrive from $-\frac{\bar{h}}{2}^\circ$ and $\frac{\bar{h}}{2}^\circ$, respectively. It is clear that the estimation performance improves with the increase of DOA separation \bar{h} .

B. Wideband DOA estimation results

We perform DOA estimation based on a 9-sensor co-prime array with $(N_1, N_2) = (3, 4)$ in this part. The normalized frequency band of the impinging wideband signals covers the

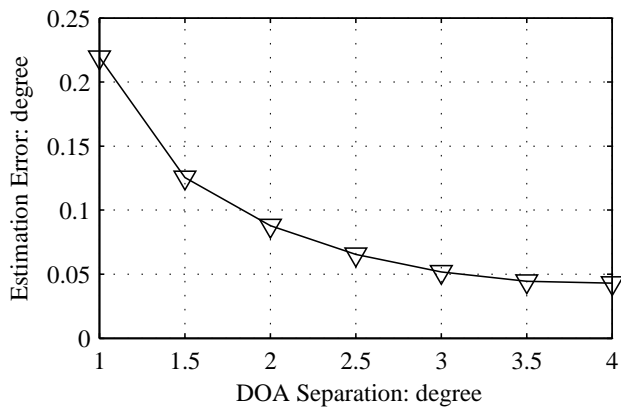


Fig. 8. RMSEs with respect to the DOA separation h between adjacent sources.

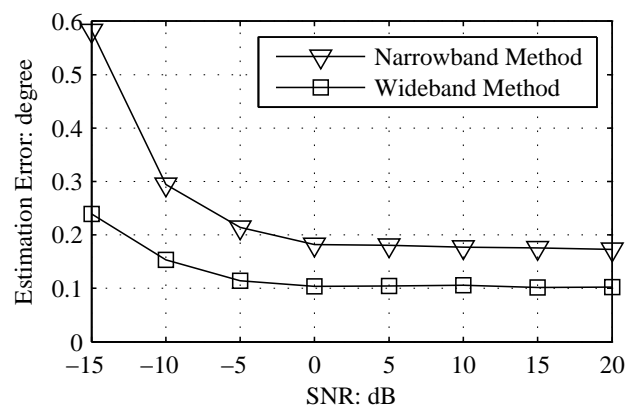
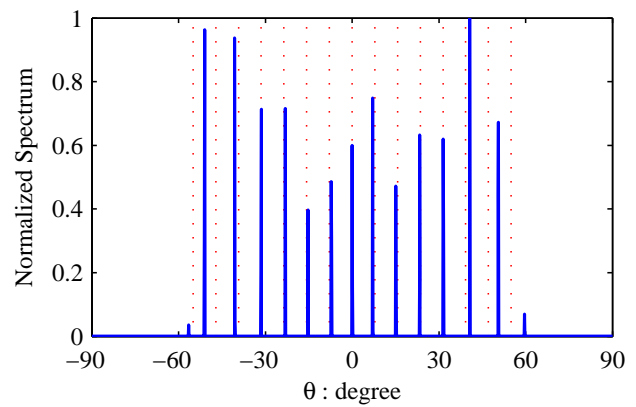


Fig. 9. RMSEs of different estimation methods versus input SNR.

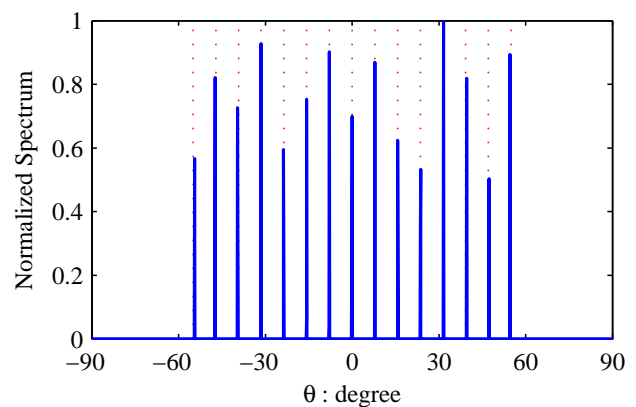
range from 0.5π to π . After applying a DFT of $L = 64$ points, there are $Q = 15$ frequency bins of interest in total with indexes from 17 to 31. The unit spacing d is equal to $\lambda_{\min}/2$, where $\lambda_{\min} = 2c/f_s$ and f_s is the sampling frequency. The number of samples in the time domain is set to be 64000. Then the number of samples P at each frequency bin is 1000. For the DOA estimation employing a single frequency bin, the best results is achieved at the highest frequency bin $l = 31$, where the relative spacing compared to signal wavelength is the largest among all frequencies of interest.

We first analyse the RMSE results with respect to a varied input SNR. There are $K = 12$ sources with incident angles uniformly distributed from -60° to 60° , and the estimation accuracy is shown in Fig. 9. We can see that the group sparsity based wideband estimation method consistently outperform the narrowband one due to exploration of all information provided by frequencies of interest simultaneously.

Then we increase the number of sources K to be 15 and let these K sources uniformly distributed from -55° to 55° to test the DOA estimation performance under a much tougher setting with reduced separation between incident angles of adjacent sources. The SNR is 0dB, and Fig. 10 gives the



(a) DOA estimation results of narrowband method for a single frequency ($l = 31$).



(b) DOA estimation results of group sparsity based wideband method.

Fig. 10. DOA estimation results of different estimation methods.

DOA estimation results obtained by the narrowband method for the single frequency ($l = 31$) and the group sparsity based wideband method. We can see that, the narrowband method clearly fails in detecting so many sources while the wideband method is capable of resolving all the sources.

Finally in this part, we analyze the performance improvement with large unit spacing co-prime array. Define $d = d_f \cdot \lambda_{\min}/2$, where d_f is the factor for adjusting the unit spacing. For $d_f > 1$, note that not all the frequency bins within the range $17 \leq l_q \leq 31$ satisfy the relationship of $d \leq \lambda_{l_q}/2$. We fix the SNR at 0dB and study the performance improvement versus d_f with the RMSE results shown in Fig. 11. In this example where the normalized frequency range is from 0.5π to π , the maximum wavelength within the frequency range satisfies $\lambda_{\max} = 2\lambda_{\min}$, and $d = \lambda_{\max}/2$ corresponds to $d_f = 2$. Then we can expect that a good performance should still be obtained at $d_f = 2$, as verified in Fig. 11. As well known, the increase in d will lead to a larger physical aperture corresponding to a higher accuracy. On the other hand, aliasing problems at all frequencies when $d \geq \lambda_{\max}/2$ will result in a more difficult DOA estimation problem. Therefore, a threshold is expected that the performance improvement introduced by

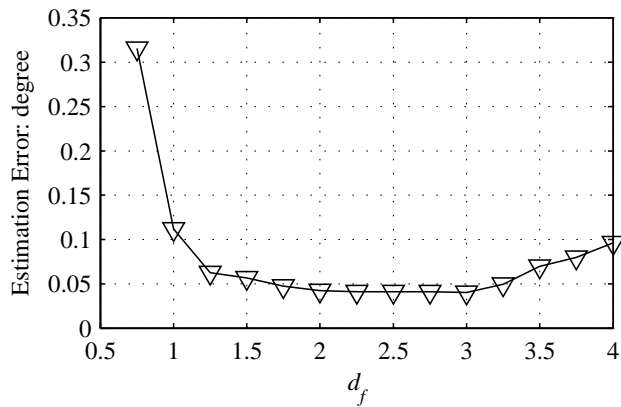


Fig. 11. RMSEs versus the unit spacing adjustment factor d_f .

the increased aperture will be offset by the loss caused by increased difficulty when d beyond the threshold. As shown in Fig 11, a better performance is achieved for about $2 \leq d_f \leq 3$, where the performance is quite flat, indicating that $d_f = 2$ corresponding to $d = \lambda_{\max}/2$ is a reasonable choice.

C. Wideband DOA estimation results for a single ULA

Consider a 9-sensor ULA with $\delta = 1$, and DFT of $L = 64$ points is applied. For the transmitted LFM CW signal, the initial frequency, time-offset, and phase are set to be 0, and the modulation period $T = 64/f_s$. To simplify the selection the frequency pairs, we set the bandwidth of interest cover $Q = 10$ frequency bins with indexes given in the set $\Phi_l = \{1, 2, \dots, 10\}$. All these 10 frequency bins are divided into $M = 5$ pairs with 1 and 10, 2 and 9, 3 and 8, 4 and 7, as well as 5 and 6.

In the first set of simulations for wideband DOA estimation employing a single ULA, we compare the estimation accuracy based on a single frequency pair and multiple frequency pairs. With $K = 20$, Fig. 12 gives the RMSE results obtained by different methods with respect to input SNR, where one pair consisting of the 5-th and 6-th frequency bins are exploited in the single frequency pair based method. It is clear that the method based on multiple pairs of frequency bins consistently outperforms the one exploiting only a single co-prime frequency pair by a big margin.

Then we give an example where the DOA estimation method for a single frequency pair clearly fails while the one with multiple frequency pairs can still obtain good results. The setting is the same as the first set except that now there are $K = 40$ targets. The SNR is set to be 0 dB, and the results are shown in Fig. 13, which again verifies the superior performance of the wideband method by jointly exploiting the information provided by multiple frequency pairs simultaneously due to the same shared spatial distribution. Furthermore, with the same number of physical sensors, a larger number of detectable sources is achieved compared with the nested array

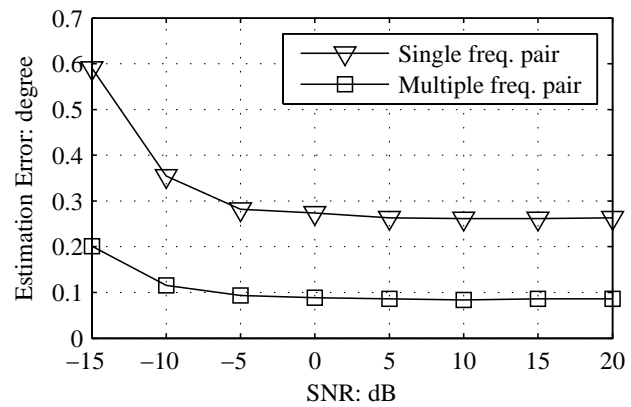
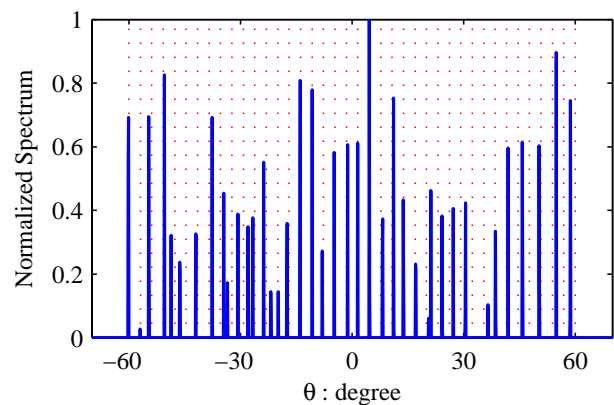
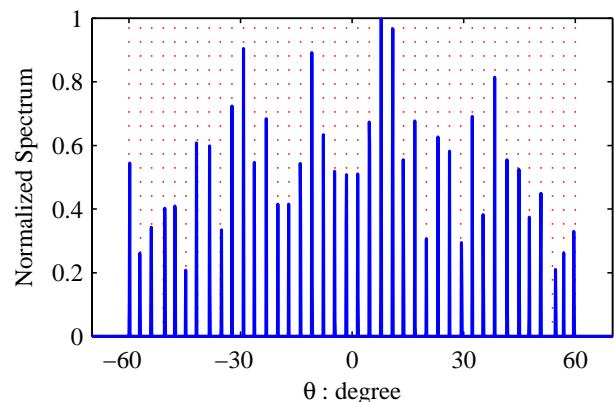


Fig. 12. RMSEs of different estimation methods versus input SNR.



(a) Estimation results for a single frequency pair (the 5-th and 6-th frequency bins).



(b) Estimation results for multiple frequency pairs.

Fig. 13. DOA estimation results obtained by different number of frequency pairs.

structure and the co-prime array structure.

VI. CONCLUSION

A review for compressive-sensing based underdetermined DOA estimation methods recently proposed in literature has been provided. The most general time-domain approach for narrowband arrays with single data snapshot and multiple

snapshots was presented first, followed by covariance matrix based approaches for multiple snapshots with a focus on underdetermined DOA estimation based on the difference co-array concept. Two specifically designed sparse structures, namely two-level nested arrays and co-prime arrays, were introduced in this context with optimized virtual sensor positions corresponding to the difference co-array. We then moved to the wideband DOA estimation problem by employing the group sparsity concept, where it has been shown that improved performance can be achieved by allowing a large unit spacing. Finally, for a specifically designed ULA structure, group sparsity based signal reconstruction method is employed for DOA estimation across the multiple frequency pairs, with a large number of DOFs achieved. Representative simulation results for typical scenarios were provided, all showing that the CS-based approach can provide an effective solution to the traditionally very difficult underdetermined DOA estimation problem.

REFERENCES

- [1] H. Krim and M. Viberg, "Two decades of array signal processing research: the parametric approach," *IEEE Signal Process. Mag.*, vol. 13, no. 4, pp. 67–94, Jul. 1996.
- [2] L. C. Godara, "Application of antenna arrays to mobile communications, part ii: Beam-forming and direction-of-arrival estimation," *Proceedings of the IEEE*, vol. 85, no. 8, pp. 1195–1245, August 1997.
- [3] H. L. Van Trees, *Optimum Array Processing, Part IV of Detection, Estimation, and Modulation Theory*. New York: Wiley, 2002.
- [4] T. E. Tuncer and B. Friedlander, *Classical and modern direction-of-arrival estimation*. New York: Academic Press, 2009.
- [5] R. O. Schmidt, "Multiple emitter location and signal parameter estimation," *IEEE Trans. Antennas Propag.*, vol. 34, no. 3, pp. 276–280, Mar. 1986.
- [6] R. Roy and T. Kailath, "ESPRIT-estimation of signal parameters via rotational invariance techniques," *IEEE Trans. Acoust., Speech, Signal Process.*, vol. 37, no. 7, pp. 984–995, Jul. 1989.
- [7] M. Boizard, G. Ginolhac, F. Pascal, S. Miron, and P. Forster, "Numerical performance of a tensor MUSIC algorithm based on HOSVD for a mixture of polarized sources," in *Proc. European Signal Processing Conference (EUSIPCO)*, 2013, pp. 1–5.
- [8] M. Haardt, F. Roemer, and G. Del Galdo, "Higher-order SVD-based subspace estimation to improve the parameter estimation accuracy in multidimensional harmonic retrieval problems," *IEEE Trans. Signal Process.*, vol. 56, no. 7, pp. 3198–3213, Jun. 2008.
- [9] F. Wen and H. C. So, "Tensor-MODE for multi-dimensional harmonic retrieval with coherent sources," *Signal Processing*, vol. 108, pp. 530–534, 2015.
- [10] B. Liao, S.-C. Chan, L. Huang, and C. Guo, "Iterative methods for subspace and DOA estimation in nonuniform noise," *IEEE Trans. Signal Process.*, vol. 64, no. 12, pp. 3008–3020, Jun. 2016.
- [11] G. Su and M. Morf, "The signal subspace approach for multiple wide-band emitter location," *IEEE Trans. Acoust., Speech, Signal Process.*, vol. 31, no. 6, pp. 1502–1522, Dec. 1983.
- [12] H. Wang and M. Kaveh, "Coherent signal-subspace processing for the detection and estimation of angles of arrival of multiple wide-band sources," *IEEE Trans. Acoust., Speech, Signal Process.*, vol. 33, no. 4, pp. 823–831, Aug. 1985.
- [13] Y.-S. Yoon, L. M. Kaplan, and J. H. McClellan, "TOPS: new DOA estimator for wideband signals," *IEEE Trans. Signal Process.*, vol. 54, no. 6, pp. 1977–1989, Jun. 2006.
- [14] D. L. Donoho, "Compressed sensing," *IEEE Trans. Inf. Theory*, vol. 52, no. 4, pp. 1289 – 1306, 2006.
- [15] E. J. Candès and M. B. Wakin, "An introduction to compressive sampling," *IEEE Signal Process. Mag.*, vol. 25, no. 2, pp. 21–30, 2008.
- [16] D. Malioutov, M. Çetin, and A. S. Willsky, "A sparse signal reconstruction perspective for source localization with sensor arrays," *IEEE Trans. Signal Process.*, vol. 53, no. 8, pp. 3010–3022, Aug. 2005.
- [17] Z.-M. Liu, Z.-T. Huang, and Y.-Y. Zhou, "Direction-of-arrival estimation of wideband signals via covariance matrix sparse representation," *IEEE Trans. Signal Process.*, vol. 59, no. 9, pp. 4256–4270, Sep. 2011.
- [18] P. Stoica, P. Babu, and J. Li, "Spice: A sparse covariance-based estimation method for array processing," *IEEE Trans. Signal Process.*, vol. 59, no. 2, pp. 629–638, Feb. 2011.
- [19] K. Lee, Y. Bresler, and M. Junge, "Subspace methods for joint sparse recovery," *IEEE Trans. Inf. Theory*, vol. 58, no. 6, pp. 3613–3641, Jun. 2012.
- [20] Z.-M. Liu, Z.-T. Huang, and Y.-Y. Zhou, "Sparsity-inducing direction finding for narrowband and wideband signals based on array covariance vectors," *IEEE Trans. Wireless Commun.*, vol. 12, no. 8, pp. 3896–3906, Aug. 2013.
- [21] H. X. Yu, X. F. Qiu, X. F. Zhang, C. H. Wang, and G. Yang, "Two-dimensional direction of arrival (DOA) estimation for rectangular array via compressive sensing trilinear model," *International Journal of Antennas and Propagation*, vol. 2015, 2015.
- [22] Z. B. Shen, C. X. Dong, Y. Y. Dong, G. Q. Zhao, and L. Huang, "Broadband DOA estimation based on nested arrays," *International Journal of Antennas and Propagation*, vol. 2015, 2015.
- [23] G. Tang and A. Nehorai, "Performance analysis for sparse support recovery," *IEEE Trans. Inf. Theory*, vol. 56, no. 3, pp. 1383–1399, Mar. 2010.
- [24] J. Yin and T. Chen, "Direction-of-arrival estimation using a sparse representation of array covariance vectors," *IEEE Trans. Signal Process.*, vol. 59, no. 9, pp. 4489–4493, Sep. 2011.
- [25] M. Carlini, P. Rocca, G. Oliveri, F. Viani, and A. Massa, "Directions-of-arrival estimation through bayesian compressive sensing strategies," *IEEE Trans. Antennas Propag.*, vol. 61, no. 7, pp. 3828–3838, 2013.
- [26] J. M. Kim, O. K. Lee, and J. C. Ye, "Compressive music: revisiting the link between compressive sensing and array signal processing," *IEEE Trans. Inf. Theory*, vol. 58, no. 1, pp. 278–301, Jan. 2012.
- [27] J. Zheng and M. Kaveh, "Sparse spatial spectral estimation: a covariance fitting algorithm, performance and regularization," *IEEE Trans. Signal Process.*, vol. 61, no. 11, pp. 2767–2777, Jun. 2013.
- [28] P. Chevalier, L. Albera, A. Férréol, and P. Comon, "On the virtual array concept for higher order array processing," *IEEE Trans. Signal Process.*, vol. 53, no. 4, pp. 1254–1271, Apr. 2005.
- [29] W.-K. Ma, T.-H. Hsieh, and C.-Y. Chi, "DOA estimation of quasi-stationary signals with less sensors than sources and unknown spatial noise covariance: a khatri-rao subspace approach," *IEEE Trans. Signal Process.*, vol. 58, no. 4, pp. 2168–2180, Apr. 2010.
- [30] D. Feng, M. Bao, Z. Ye, L. Guan, and X. Li, "A novel wideband doa estimator based on khatri-rao subspace approach," *Signal Processing*, vol. 91, no. 10, pp. 2415–2419, Apr. 2011.
- [31] A. Moffet, "Minimum-redundancy linear arrays," *IEEE Trans. Antennas Propag.*, vol. 16, no. 2, pp. 172–175, Mar. 1968.
- [32] R. T. Hoctor and S. A. Kassam, "The unifying role of the coarray in aperture synthesis for coherent and incoherent imaging," *Proc. IEEE*, vol. 78, no. 4, pp. 735–752, Apr. 1990.
- [33] J.-F. Cardoso and E. Moulines, "Asymptotic performance analysis of direction-finding algorithms based on fourth-order cumulants," *IEEE Trans. Signal Process.*, vol. 43, no. 1, pp. 214–224, Jan. 1995.
- [34] M. B. Hawes and W. Liu, "Sparse array design for wideband beamforming with reduced complexity in tapped delay-lines," *IEEE Trans. Audio, Speech and Language Processing*, vol. 22, pp. 1236–1247, August 2014.
- [35] —, "Design of fixed beamformers based on vector-sensor arrays," *International Journal of Antennas and Propagation*, vol. 2015, 2015.
- [36] P. Pal and P. P. Vaidyanathan, "Nested arrays: a novel approach to array processing with enhanced degrees of freedom," *IEEE Trans. Signal Process.*, vol. 58, no. 8, pp. 4167–4181, Aug. 2010.
- [37] P. P. Vaidyanathan and P. Pal, "Sparse sensing with co-prime samplers and arrays," *IEEE Trans. Signal Process.*, vol. 59, no. 2, pp. 573–586, Feb. 2011.

- [38] P. Pal and P. P. Vaidyanathan, "Coprime sampling and the MUSIC algorithm," in *Proc. IEEE Digital Signal Processing Workshop and IEEE Signal Processing Education Workshop (DSP/SPE)*, Sedona, AZ, Jan. 2011, pp. 289–294.
- [39] K. Han and A. Nehorai, "Improved source number detection and direction estimation with nested arrays and ulas using jackknifing," *IEEE Trans. Signal Process.*, vol. 61, no. 23, pp. 6118–6128, Dec. 2013.
- [40] —, "Nested array processing for distributed sources," *IEEE Signal Process. Lett.*, vol. 21, no. 9, pp. 1111–1114, Sep. 2014.
- [41] Y. D. Zhang, M. G. Amin, and B. Himed, "Sparsity-based DOA estimation using co-prime arrays," in *Proc. IEEE International Conference on Acoustics, Speech and Signal Processing (ICASSP)*, Vancouver, Canada, May 2013, pp. 3967–3971.
- [42] Y. D. Zhang, M. G. Amin, F. Ahmad, and B. Himed, "DOA estimation using a sparse uniform linear array with two CW signals of co-prime frequencies," in *Proc. IEEE International Workshop on Computational Advances in Multi-Sensor Adaptive Processing*, Saint Martin, Dec. 2013, pp. 404–407.
- [43] Q. Shen, W. Liu, W. Cui, S. Wu, Y. D. Zhang, and M. G. Amin, "Group sparsity based wideband DOA estimation for co-prime arrays," in *Proc. IEEE China Summit and International Conference on Signal and Information Processing (ChinaSIP)*, Xi'an, China, Jul. 2014, pp. 252–256.
- [44] Q. Shen, W. Liu, W. Cui, and S. Wu, "Low-complexity compressive sensing based DOA estimation for co-prime arrays," in *Proc. International Conference on Digital Signal Processing*, Hong Kong, China, Aug. 2014, pp. 754–758.
- [45] S. Qin, Y. D. Zhang, and M. G. Amin, "Generalized coprime array configurations for direction-of-arrival estimation," *IEEE Transactions on Signal Processing*, vol. 63, no. 6, pp. 1377–1390, March 2015.
- [46] P. Pal and P. Vaidyanathan, "Pushing the limits of sparse support recovery using correlation information," *IEEE Trans. Signal Process.*, vol. 63, no. 3, pp. 711–726, Feb. 2015.
- [47] E. BouDaher, F. Ahmad, and M. G. Amin, "Sparsity-based direction finding of coherent and uncorrelated targets using active nonuniform arrays," *IEEE Signal Process. Lett.*, vol. 22, no. 10, pp. 1628–1632, Oct. 2015.
- [48] C.-L. Liu and P. Vaidyanathan, "Super nested arrays: Linear sparse arrays with reduced mutual coupling-part i: Fundamentals," *IEEE Trans. Signal Process.*, vol. 64, no. 15, pp. 3997–4012, Aug. 2016.
- [49] C.-L. Liu and P. P. Vaidyanathan, "Super nested arrays: Linear sparse arrays with reduced mutual coupling-part ii: High-order extensions," *IEEE Trans. Signal Process.*, vol. 64, no. 16, pp. 4203–4217, Aug. 2016.
- [50] P. Pal and P. Vaidyanathan, "Multiple level nested array: An efficient geometry for 2qth order cumulant based array processing," *IEEE Trans. Signal Process.*, vol. 60, no. 3, pp. 1253–1269, Mar. 2012.
- [51] Q. Shen, W. Liu, W. Cui, and S. Wu, "Extension of nested arrays with the fourth-order difference co-array enhancement," in *Proc. IEEE International Conference on Acoustics, Speech and Signal Processing (ICASSP)*, Shanghai, China, Mar. 2016, pp. 2991–2995.
- [52] —, "Extension of co-prime arrays based on the fourth-order difference co-array concept," *IEEE Signal Process. Lett.*, vol. 23, no. 5, pp. 615–619, May 2016.
- [53] Q. Shen, W. Liu, W. Cui, S. Wu, Y. D. Zhang, and M. G. Amin, "Low-complexity direction-of-arrival estimation based on wideband co-prime arrays," *IEEE/ACM Trans. Audio, Speech, Language Process.*, vol. 23, no. 9, pp. 1445–1456, Sep. 2015.
- [54] S. Qin, Y. D. Zhang, and M. G. Amin, "DOA estimation exploiting coprime frequencies," in *Proc. SPIE Wireless Sensing, Localization, and Processing IX*, vol. 9103, Baltimore, MD, May 2014, p. 91030E.
- [55] E. BouDaher, F. Ahmad, and M. G. Amin, "Sparse reconstruction for direction-of-arrival estimation using multi-frequency co-prime arrays," *EURASIP Journal on Advances in Signal Processing*, vol. 2014, pp. 1–11, 2014.
- [56] E. BouDaher, Y. Jia, F. Ahmad, and M. G. Amin, "Multi-frequency co-prime arrays for high-resolution direction-of-arrival estimation," *IEEE Trans. Signal Process.*, vol. 63, no. 14, pp. 3797–3808, Jul. 2015.
- [57] S. Qin, Y. D. Zhang, M. G. Amin, and B. Himed, "DOA estimation exploiting a uniform linear array with multiple co-prime frequencies," *Signal Processing*, vol. 130, pp. 37–46, Jan. 2017.
- [58] Q. Shen, W. Liu, W. Cui, S. Wu, Y. D. Zhang, and M. G. Amin, "Wideband DOA estimation for uniform linear arrays based on the co-array concept," in *Proc. European Signal Processing Conference (EUSIPCO)*, Nice, France, Sep. 2015, pp. 2885–2889.
- [59] Y. Chi, L. L. Scharf, A. Pezeshki *et al.*, "Sensitivity to basis mismatch in compressed sensing," *IEEE Trans. Signal Process.*, vol. 59, no. 5, pp. 2182–2195, May 2011.
- [60] H. Zhu, G. Leus, and G. B. Giannakis, "Sparsity-cognizant total least-squares for perturbed compressive sampling," *IEEE Trans. Signal Process.*, vol. 59, no. 5, pp. 2002–2016, May 2011.
- [61] Z. Yang, C. Zhang, and L. Xie, "Robustly stable signal recovery in compressed sensing with structured matrix perturbation," *IEEE Trans. Signal Process.*, vol. 60, no. 9, pp. 4658–4671, Sep. 2012.
- [62] Z. Yang, L. Xie, and C. Zhang, "Off-grid direction of arrival estimation using sparse bayesian inference," *IEEE Trans. on Signal Process.*, vol. 61, no. 1, pp. 38–43, Jan. 2013.
- [63] Z. Tan and A. Nehorai, "Sparse direction of arrival estimation using co-prime arrays with off-grid targets," *IEEE Signal Process. Lett.*, vol. 21, no. 1, pp. 26–29, Jan. 2014.
- [64] Z. Tan, P. Yang, and A. Nehorai, "Joint sparse recovery method for compressed sensing with structured dictionary mismatches," *IEEE Trans. Signal Process.*, vol. 62, no. 19, pp. 4997–5008, Oct. 2014.
- [65] Q. Shen, W. Cui, W. Liu, S. Wu, Y. D. Zhang, and M. G. Amin, "Underdetermined wideband DOA estimation of off-grid sources employing the difference co-array concept," *Signal Processing*, vol. 130, pp. 299–304, 2017.
- [66] E. J. Candès, J. Romberg, and T. Tao, "Robust uncertainty principles: Exact signal reconstruction from highly incomplete frequency information," *IEEE Trans. Inf. Theory*, vol. 52, no. 2, pp. 489–509, Feb. 2006.
- [67] E. J. Candès, M. B. Wakin, and S. P. Boyd, "Enhancing sparsity by reweighted l_1 minimization," *Journal of Fourier Analysis and Applications*, vol. 14, pp. 877–905, 2008.
- [68] G. Prisco and M. D'Urso, "Maximally sparse arrays via sequential convex optimizations," *IEEE Antennas and Wireless Propagation Letters*, vol. 11, pp. 192–195, February 2012.
- [69] B. Fuchs, "Synthesis of sparse arrays with focused or shaped beam-pattern via sequential convex optimizations," *IEEE Transactions on Antennas and Propagation*, vol. 60, no. 7, pp. 3499–3503, May 2012.
- [70] M. B. Hawes and W. Liu, "Compressive sensing based approach to the design of linear robust sparse antenna arrays with physical size constraint," *IET Microwaves, Antennas & Propagation*, vol. 8, pp. 736–746, July 2014.
- [71] C.-L. Liu and P. Vaidyanathan, "Cramér–rao bounds for coprime and other sparse arrays, which find more sources than sensors," *Digital Signal Processing*, 2016.
- [72] A. Koochakzadeh and P. Pal, "Cramér–rao bounds for underdetermined source localization," *IEEE Signal Process. Lett.*, vol. 23, no. 7, pp. 919–923, 2016.
- [73] M. Grant and S. Boyd. (2013, Dec.) CVX: Matlab software for disciplined convex programming, version 2.0 beta, build 1023. [Online]. Available: <http://cvxr.com/cvx>
- [74] —, "Graph implementations for nonsmooth convex programs," in *Recent Advances in Learning and Control*, ser. Lecture Notes in Control and Information Sciences, V. Blondel, S. Boyd, and H. Kimura, Eds. Springer-Verlag, 2008, pp. 95–110, http://stanford.edu/~boyd/graph_dcp.html.